第 27 卷第 10 期 无 机 化 学 学 报 Vol.27 No.10
2011 年 10 月 CHINESE JOURNAL OF INORGANIC CHEMISTRY 2033-2038

超声波辐射快速合成高光催化性能的 BiOCl(Br)纳米片

余长林*,[1] 周晚琴[2] YU Jimmy C[3]
([1]江西理工大学冶金与化学工程学院)
([2]江西理工大学信息工程学院,赣州 341000)
([3]香港中文大学化学系,香港)

摘要: 在室温条件下,利用超声波辐射方法快速合成了四方状 BiOCl(BiOBr)纳米片光催化剂。应用 N_2-物理吸附、X 射线粉末衍射、扫描电镜、透射电镜、紫外可见光谱等手段对催化剂进行了表征,并以波长为 λ=365 nm 的紫外光和 420 nm<λ<660 nm 的可见光为光源,评价了该催化剂光催化降解酸性橙Ⅱ的活性。表征结果表明,超声波辐射可加速 BiOCl 和 BiOBr 晶化过程,显著提高 BiOCl 和 BiOBr 的结晶度,并使其晶粒发生细化,提高催化剂的比表面积。活性测试表明,声化学合成样品的光催化活性优于普通搅拌制备的样品。其中 BiOCl 的紫外光催化活性高于商业 TiO_2(P25)光催化剂。

关键词: 超声波辐射; BiOCl; BiOBr; 纳米片; 光催化; 酸性橙Ⅱ
中图分类号: TB321; O643 **文献标识码**: A **文章编号**: 1001-4861(2011)10-2033-06

Rapid Fabrication of BiOCl(Br) Nanosheet with High Photocatalytic Performance via Ultrasound Irradiation

YU Chang-Lin*,[1] ZHOU Wan-Qin[2] YU Jimmy C[3]
([1]*School of Metallurgy and Chemical Engineering, [2]School of Information Engineering, Jiangxi University of Science and Technology, Ganzhou, Jiangxi* 341000, *China*)
([3]*Department of Chemistry, The Chinese University of Hong Kong, Hong Kong, China*)

Abstract: Square-like BiOCl and BiOBr nanosheets with high crystallinity were rapidly fabricated by ultrasound irradiation . The prepared samples were characterized by N_2 physical adsorption, X-ray diffraction (XRD), scanning electron microscopy (SEM), transmission electron microscopy (TEM), and UV-Vis diffuse reflectance spectroscopy (UV-Vis DRS). The photocatalytic activity of the samples was evaluated by photocatalytic degradation of acid orange Ⅱ under both UV light (λ=365 nm) and visible light (420 nm<λ<660 nm) irradiation. Ultrasound irradiation could effectively accelerate the crystallization process of the BiOCl and BiOBr, increase the surface areas of the samples, and decrease the size of the grain. Much higher photocatalytic activity could be obtained over sonochemistry synthesized samples than the samples prepared by common stirring method. Under UV light irradiation, the activity of sonochemistry synthesized BiOCl is superior to that of commercial TiO_2 (P25, Degussa).

Key words: ultrasound irradiation; BiOCl and BiOBr; nanosheet; photocatalysis; acid orange Ⅱ

Nowadays, semiconductor photocatalysis has received intensive attention in environmental purification due to its simplicity, mild reaction condition and low energy consumption [1-5]. Bismuth oxyhalides, BiOX (X=Cl, Br, I), have broad industrial applications as ferroelectric materials and pigments.

收稿日期:2011-04-26。收修改稿日期:2011-06-19。
国家自然科学基金(No.21067004),江西省自然科学基金(2010GZH0048),厦门大学固体表面物理化学国家重点实验室开放基金(200906)资助项目。
*通讯联系人。E-mail:yuchanglinjx@163.com

Recently, the performances of bismuth oxyhalides in photocatalytic degradation of organic compounds have aroused much attention [6-12]. Zhang and co-workers [6] reported that BiOCl exhibited high performance in photocatalytic degradation of methyl orange (MO) dye. A very high photocatalytic activity in the degradation of MO under visible light irradiation was observed for BiOI microspheres[7]. Lin et al.[10] also reported that the photocatalytic activity of Bi_3O_4Cl synthesized by a solid-state reaction of BiOCl and Bi_2O_3 was higher than that of anatase-type TiO_2 under UV light illumination for degrading MO. Our research indicates the deposition of Ag nano-particles over BiOBr could bring a very high efficiency in decomposition of dyes [11]. However, the photocatalytic performance of the bismuth oxyhalides is mainly dependent on its microstructure, such as the crystal phase, particle size and morphology [7,12]. The microstructure of the catalyst is mainly determined by its preparation method.

Sonochemical processing has been proven to be a unique and effective method to synthesize nanostructure materials at low temperature, such as ZnO nanorods[13], TiO_2 microspheres [14], $PbWO_4$ [15], Te nanorods [16], CuO doped $BiVO_4$ crystals[17]. The effects of acoustic cavitation from the ultrasound irradiation in a liquid could produce the extreme conditions, such as the extremely high temperatures (~5 000 ℃). This specific physical chemistry environment will benefit the dissolution of chemical bond, collision and exchange of atom and ion, and the crystallization of semiconductor.

We report here the effect of ultrasound irradiation on the structure and photocatalytic performance of BiOCl and BiOBr in degradation of acid orange Ⅱ.

1 Experimental

1.1 Catalyst synthesis

All chemicals with analytical grade were obtained from Sinopharm Chemical Reagent Co. Ltd. and were used as received without further purification. In a typical experiment to prepare the BiOCl (BiOBr) sample by sonochemistry, 0.01 mol $Bi(NO_3)_3 \cdot 5H_2O$ powders were firstly dissolved in 15 mL glacial acetic acid to obtain solution A. 0.01 mol NaCl(NaBr) and 0.02 mol CH_3COONa were dissolved in 200 mL deionized water to obtain solution B. Under sonication, solution A was added dropwise to solution B. After the completion of solution A addition, the mixture was exposed to powerful ultrasonic irradiation for 10 min under ambient air. This high-intensity ultrasound irradiation was accomplished with a high-intensity ultrasonic probe (Xinzhi Co., Xinzhi, China; 20 kHz; 2 cm diameter; Ti-horn; 20 kHz; 800 $W \cdot cm^{-2}$) immersed directly in the reaction solution. During the whole process, the sonication cell was water-cooled to maintain the temperature at around 25 ℃. The obtained precipitate was centrifuged, washed with deionized water and finally dried in air at 100 ℃. To investigate the influence of the preparation conditions on the structure property of the samples, the conventional method was also used to prepare corresponding samples[8-9].

1.2 Catalyst characterization

The Brunauer-Emmett-Teller (BET) surface areas of the samples were obtained from N_2 adsorption/desorption isotherms determined at liquid nitrogen temperature (77 K) on an automatic analyzer (NOVA 4000). The samples were outgassed for 2 h under vacuum at 350 ℃ prior to adsorption. X-ray diffraction (XRD) patterns were obtained on a Bruker D8 Advance X-ray diffractometer using Cu $K\alpha$ radiation (λ=0.154 178 nm) at a scan rate of $0.05°(2\theta) \cdot s^{-1}$. The accelerating voltage and the applied current were 40 kV and 15 mA, respectively. The total morphology of the samples were determined by a XL30 (Philips) scanning electron microscope (SEM). UV-Vis diffuse reflectance spectra (DRS) were recorded using a UV-Vis spectrophotometer (UV-2550, Shimadzu). To investigate the microstructure of the prime particle of the sample, transmission electron microscopy (TEM) was performed using a CM-120 microscope (Philips, 120 kV).

1.3 Photocatalytic activity test

The photocatalytic activities of the samples were determined by measuring the degradation of acid orange Ⅱ in an aqueous solution under both UV light and visible light irradiation. In UV light activity test, a 365 nm UV lamp (15 W Cole-Parmer Instrument Co.) was used as light source. The photocatalyst (0.05 g) was

suspended in 80 mL aqueous solution of C_0=0.020 g·L^{-1}. Before the lamp was turned on, the suspension was stirred in the dark for 40 min. The suspension was vigorously stirred in the photoreactor during the process and the temperature of suspension was maintained at around 25 ℃ by the circulation of water through an external cooling coil. After fixed intervals of illumination, a sample of the suspension was taken out and centrifuged. The clear upper layer solution was analyzed by a spectrophotometer (UV-2550, Shimadzu). The dye concentration was measured at λ of 484 nm. The degradation rate (D) of acid orange Ⅱ was calculated according to the equation: $D=(A_0-A)/A_0\times 100\%$ (A_0: initial absorption degree; A: final absorption degree). In visible light activity test, a 100 W tungsten lamp was positioned inside a cylindrical Pyrex vessel surrounded by a circulating cooling water jacket and a cutoff filter solution jacket HCl aqueous solution of $CuSO_4$ (0.5 mol·L^{-1}) and K_2CrO_4 (0.002 mol·L^{-1}) whose cuts off wavelength is shorter than 400 nm and longer than 660 nm[18].

2 Results and discussion

2.1 Characterization analysis

2.1.1 XRD analysis

Fig.1 shows the XRD patterns of the BiOCl and BiOBr samples prepared under different conditions. As to the BiOCl sample, ultrasonic irradiation causes very strong reflection peaks at 2θ=10.76°, 21.69°, 24.98°, 31.43°, 31.97°, 39.00°, 46.09°, 50.46° and 56.91°. These reflection peaks correspond to the planes of (001), (002), (011), (012), (110), (112), (020), (014) and (212), respectively, which can be readily indexed to the tetragonal phase of BiOCl [space group: *P*4/*nmm* (129)] (corresponding PDF No. 73-2060). No impurities can be detected from this pattern of BiOCl. Compared with the sonicated BiOCl, only weak reflection peaks are observed for the BiOCl obtained by stirring 24 h. Similar changes are observed for BiOBr samples prepared under different conditions. The XRD analysis demonstrates that BiOCl and BiOBr with high crystallinity can be fast prepared by powerful ultrasonic irradiation at low temperature. The extreme chemical conditions arising from acoustic cavitation could accelerate the formation of BiOCl and BiOBr crystals because the transient high-temperature (~5 000 ℃) and high-pressure (>20 MPa) field produced during ultrasound irradiation could provide a favorable environment for the crystallization process of the amorphous BiOCl and BiOBr. Furthermore, the energy generated during collision can induce the crystallization of the amorphous particles.

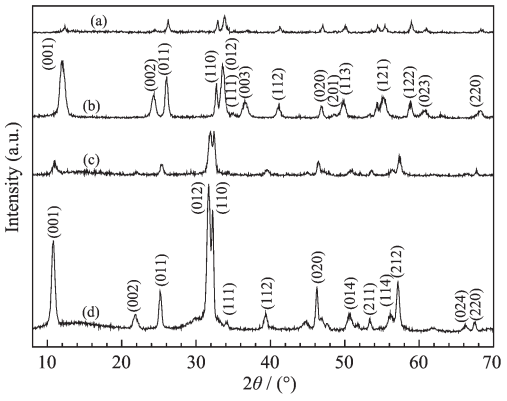

(a) BiOCl stirred for 24 h; (b) BiOCl sonicated for 10 min; (c) BiOBr stirred for 24 h; (d) BiOBr sonicated for 10 min

Fig.1 XRD patterns of the samples prepared under different conditions

From the plane of (001), the Scherrer equation was applied to estimate the average crystallite sizes of the samples: $d=0.89\lambda/B(2\theta)\cos\theta$, where $B(2\theta)$ is the width of the XRD peak at half peak-height in radian, λ is the wavelength of the X-ray in nanometer (λ = 0.154 nm), θ is the angle between the incident and diffracted beams in degree, and d is the average crystallite size of the powder sample in nanometer. The calculation shows that the average crystalline sizes for the BiOCl and BiOBr prepared under stirring condition are 28 and 17 nm, respectively. However, as for BiOCl and BiOBr prepared under sonicating condition the average crystalline sizes are 10.78 and 15.38. It is obviously that ultrasonic irradiation could effectively decrease the average crystalline size.

2.1.2 Microstructures analysis

The effects of ultrasound irradiation on the total morphology and dispersion of the samples were analyzed by SEM. From Fig.2, it can be seen that the BiOCl sample prepared by conventional method is

composed of a large quantity of relatively thick sheets. Ultrasound irradiation makes these sheets become thin and well dispersed. As for the BiOBr prepared by conventional method, no very regular sheets can be observed. Some sheets aggregate into the big and flower-like clusters. However, for ultrasound prepared BiOBr, no big flower-like clusters are observed. The sample is composed of small and very uniform sheets.

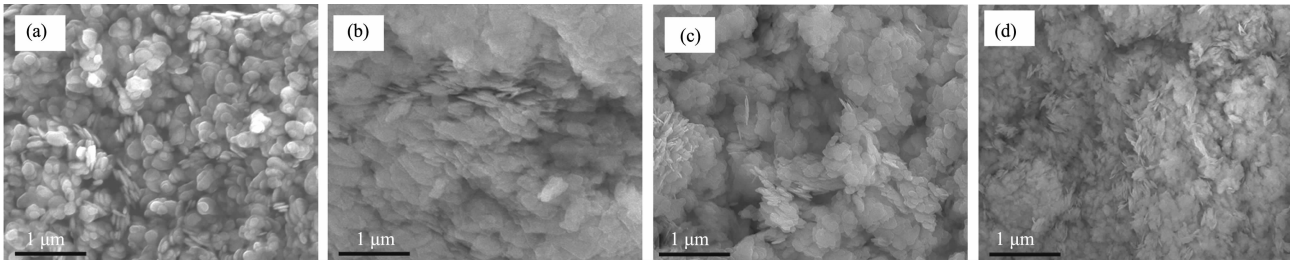

(a) BiOCl stirred for 24 h; (b) BiOCl sonicated for 10 min; (c) BiOBr stirred for 24 h; (d) BiOBr sonicated for 10 min

Fig.2 SEM images of the samples prepared under different conditions

Fig.3(a) and (b) shows the TEM photograph of BiOCl prepared by different conditions. This figure indicates that BiOCl particles prepared by stirring have square shape and smooth surface with a size of 100~120 nanometer. However, ultrasound irradiation makes these BiOCl particles shown much smaller grain size (50~80 nanometer). As to BiOBr, a similar variation appears. The analysis of SEM and TEM shows that ultrasound irradiation could make the particles become smaller and well dispersed. The good dispersion of the catalyst particle will benefit the adsorption of dye and light absorption. In addition, the BET surface area of the samples was determined by N_2 adsorption. The BET surface areas of BiOCl (conventioal stirring), BiOCl (sonicating), BiOBr (conventioal stirring), and BiOBr (sonicating), are 14, 25, 12 and 24 $m^2 \cdot g^{-1}$, respectively. Ultrasonic irradiation could increase the surface area of the catalysts. It is reasonable to infer that the high intensity ultrasound irradiation could benefit not only the crystallization of BiOCl (BiOBr) but also the formation of small and well dispersed bismuth oxyhalides particles. The diminishing of the particles could give an increase in the surface area.

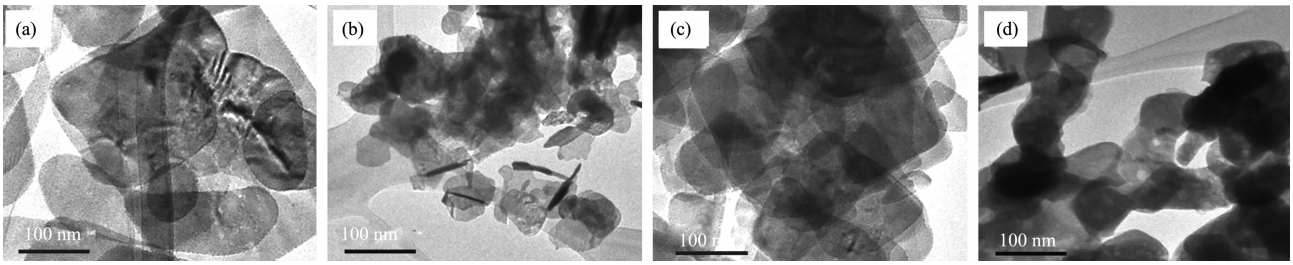

(a) BiOCl stirred for 24 h; (b) BiOCl sonicated for 10 min; (c) BiOBr stirred for 24 h; (d) BiOBr sonicated for 10 min

Fig.3 TEM images of the samples prepared under different conditions

2.1.3 UV-Vis diffuse reflectance spectra

Fig.4 shows the UV-Vis diffuse reflectance absorption spectra of all the samples prepared under different conditions. The absorption edge of BiOCl appears in the UV light region. However, BiOBr shows strong absorption in the visible region. The absorption edges for BiOCl (conventioal stirring), BiOCl (sonicating), BiOBr (conventioal stirring), and BiOBr (sonicating), are 366, 353, 447 and 440 nm, respectively. The absorption edge shows a monotonic blue shift for the sonochemistry fabricated samples. The steep shape of the absorption curve indicates that the absorption band is not ascribed to the transition from the impurity level to the conduction band, but to the intrinsic transition between the valence band and the conduction band[19-21]. The band gap energy (E_g) for the catalyst is determined with $E_g = 1\ 240/\lambda_g$ (eV) where λ_g is the absorption edge, which is obtained

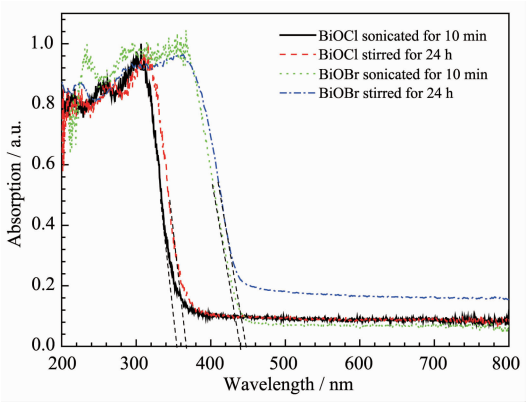

Fig.4　UV-Vis diffuse reflectance absorption spectra of all the samples

from the intercept between the tangent of the absorption curve and the abscissa[22]. The approximate band gap energies of the resulting samples are 3.39, 3.51, 2.77 and 2.82 eV for BiOCl (conventioal stirring), BiOCl (sonicating), BiOBr (conventioal stirring), and BiOBr (sonicating), at the absorption edge of 366, 353, 447 and 440 nm, respectively. The reason for the blue shift is not clear. However, it may be related to the grain refinement of the sample caused by ultrasonic irradiation.

2.2　Photocatalytic activity test

The photocatalytic activities of the samples were evaluated by measuring the decomposition of acid orange Ⅱ in an aqueous solution under both UV light (λ =365 nm) and visible light (420 nm<λ <660 nm) irradiation. Blank test shows that acid orange Ⅱ almost can not be degraded under both UV and visible light irradiation without a catalyst, indicating that acid orange Ⅱ is a stable molecule and its photolysis can be ignored.

Fig.5 (a) and (b) show the comparison of the photocatalytic activity of the samples under UV light irradiation. It can be seen that sonochemistry fabricated BiOCl shows the highest photocatalytic activity. Almost 100% degradation rate of acid orange II can be obtained after 1 h of light irradiation, which is higher than that of commercial TiO_2 (P25, Degussa). The sonochemistry fabricated BiOBr also shows the higher degradation rate (64%) than that of BiOBr (56%) prepared by conventioal stirring. A nanosized photocatalyst is often more photoactive because a fast

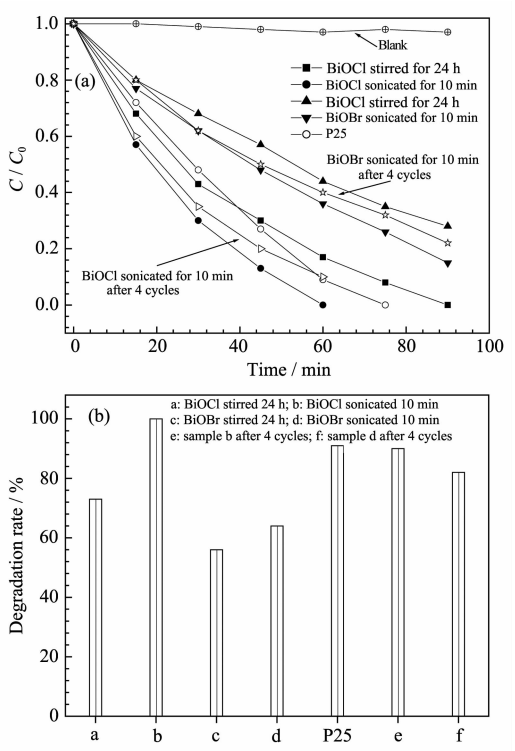

(a) Acid orange Ⅱ concentration changes as a function of time; (b) The degradation rate of Acid orange Ⅱ after 1h irradiation

Fig.5　comparison of the photocatalytic activity of the samples under UV light irradiation

electron removal can minimize electron-hole pair recombination. For example, it takes about 100 ns for electron to migrate from the interior of a 1 μm TiO_2 to its surface[24]. When the particle size shrinks to 10 nm, this process needs only about 10 ps. Moreover the increase of surface area caused by ultrasonic irradiation could promote the adsorption of dye and light absorption and the increase in crystallinity could reduce the recombination center of photo-generated electrons and holes, thus resulting in higher photocatalytic activity.

Fig.6 (a) and (b) also show the photocatalytic activity of the samples under visible light irradiation. Higher activity was also obtained over the sonochemistry fabricated BiOBr. BiOCl almost shows no activity under visible light irradiation.The process for photocatalysis is the direct absorption of photons by the band gap of the semiconductor and generates electron-hole pairs. Here, the excitation of an electron from the valence band to the conduction band is initiated by light absorption with energy equal to or

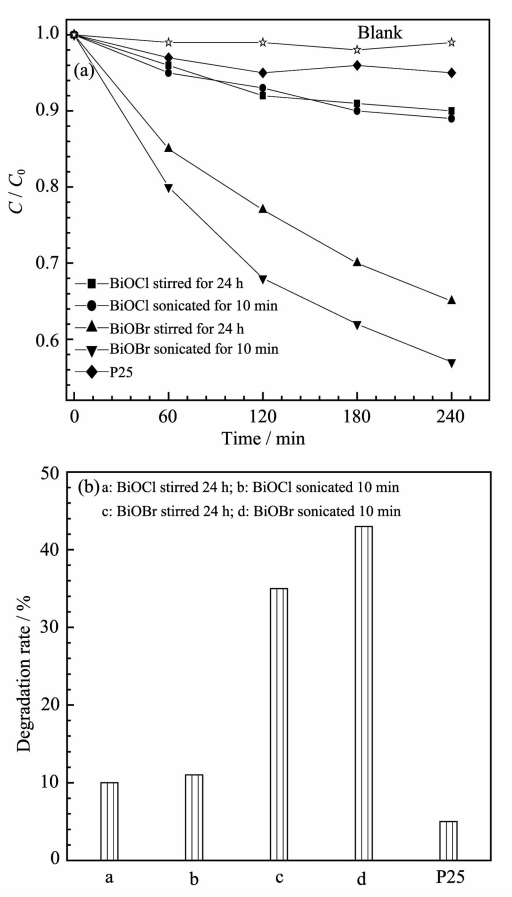

(a) Acid orange Ⅱ concentration changes as a function of time; (b) The degradation rate of Acid orange Ⅱ after 1h irradiation

Fig.6 Comparison of the photocatalytic activity of the samples prepared under visible light irradiation

greater than the band gap of the semiconductor. However, the band gap of BiOCl is 3.39~3.51 eV as mentioned earlier, which cannot absorb visible light.

3 Conclusions

The effects of the ultrasound irradiation on the structure properties of the BiOCl and BiOBr and their photocatalytic activity in the degradation of acid orange Ⅱ were investigated. It was found that much higher photocatalytic performance could be obtained over the sonochemistry fabricated samples than that of samples prepared by common stirring method. The high photocatalytic activity of the sonochemistry prepared samples could be attributed to the high crystallinity, small crystal size and larger surface area induced by ultrasound irradiation.

References:

[1] YANG Juan(杨娟), LI Jian-Tong(李建通), MIAO Juan(缪娟). *Chinese J. Inorg. Chem.* (*Wuji Huaxue Xuebao*), **2011**,**27**(3): 547-555

[2] Yu J G, Xiang Q J, Zhou M H. *Appl. Catal. B*, **2009**,**90**:595-602

[3] ZHANG Xia(张霞), MENG Hao(孟皓), CAO Xiang-Hui (曹向会). *Chinese J. Inorg. Chem.* (*Wuji Huaxue Xuebao*), **2009**,**25**(11):1947-1952

[4] Zhang M, Chen C C, Ma W H, et al. *Angew. Chem. Int. Ed.*, **2008**,**47**:9730-9733

[5] WU Yu-Ping(吴玉萍), ZHOU Zhong-Hua (周忠华), MENG Yan-Chao(孟彦超) , et al. *Chinese J. Inorg. Chem.*(*Wuji Huaxue Xuebao*), **2011**,**27**(3):473-479

[6] Zhang K L, Liu C M, Huang F Q, et al. *Appl. Catal. B*, **2006**, **68**:125-129

[7] Zhang X, Ai Z H, Jia F L, et al. *J. Phys. Chem. C*, **2008**, **112**:747-753

[8] Wang W D, Huang F Q, Lin X P, et al. *Catal. Commun.* **2008**,**9**:8-12

[9]Yu C L, Yu J C. *Mater. Sci. Eng. B*, **2010**,**166**:213-219

[10]Lin X P, Huang T, Huang F Q, et al. *J. Phys. Chem. B*, **2006**,**110**:24629-24634

[11]Yu C L, Fan C F, Meng X J, et al. *Reac. Kinet. Mech. Cat.*, **2011**,**103**:141-151

[12]Yu C L, Fan C F, Yu J C, et al. *Mater. Res. Bull.*, **2011**, **46**:140-146

[13]Jung S H, Oh E, Lee K H, et al. *Adv. Mater.*, **2007**,**19**:749-753

[14]Yu C L, Yu J C, Chan M. *J. Solid State Chem.*, **2009**,**182**: 1061-1069

[15]Geng J, Lu D J, Zhu J J, et al. *J. Phys. Chem. B*, **2006**,**110**: 13777-13785

[16]Zhu W, Wang W Z, Xu H L, et al. *J. Crystal Growth*, **2006**, **295**:69-74

[17]Yu C L, Yang K, Yu J C, et al. *J. Alloys Compd.*, **2011**, **509**:4547-4552

[18]Yu C L, Yu J M. *Catal. Lett.*, **2009**,**129**:462-470

[19]Kudo A, Sekizawa M. *Chem. Commun.*, **2000**,**15**:1371-1374

[20]Kudo A, Tsuji I, Kato H. *Chem. Commun.*, **2002**,**17**:1958-1959

[21]Lei Z, You W, Liu M, et al. *Chem. Commun.*, **2003**,**17**:2142-2142

[23]GAO Lian(高濂), ZHENG San(郑珊), ZHANG Qing-Hong (张庆红). *Nano TiO_2 Photocatalytic Materials and Application*(纳米氧化钛光催化材料及应用). Beijing: Chemical Industry Press, **2002**:110-111

[24]Lewis N S. *Annu. Rev. Phys. Chem.*, **1991**,**42**:543-580